

# A Nonlinear Method to Identify Seizure Dynamic Trajectory Based on Variance of Recurrence Rate in Human Epilepsy Patients Using EEG

## Abstract

**Background:** Surgery is a well-established treatment for drug-resistant epilepsy, but outcomes are often suboptimal, especially when no lesion is visible on preoperative imaging. A major challenge in determining the seizure's origin and spread is interpreting electroencephalogram (EEG) data. Accurately tracing the seizure's signal trajectory, given the brain's complex behavior, remains a crucial hurdle. **Materials and Methods:** In this study, EEG data from 17 patients were analyzed, using the clinical interpretations of the epileptogenic region as the gold standard. Quantification analysis of recurrence plots primarily based on variance in recurrence rate was used to identify the regions involved during seizures based on investigation of the recurrence phenomena between the regions. This method allowed for a stage-wise analysis across EEG electrodes, highlighting simultaneously involved areas. **Results:** The method effectively distinguished involved from noninvolved regions across anterior, posterior, right temporal, and left temporal areas with macro averaged F-score of 95.54. For the anterior region, it achieved an overall accuracy (correct predictions out of total predictions) of 86.96%, sensitivity (ability to correctly identify seizure-involved regions) of 82.79%, and specificity (ability to correctly identify non-involved regions) of 86.96%. For the other regions, accuracy, sensitivity, and specificity values ranged from 66.0% to 89.13%. **Conclusions:** This approach could pinpoint brain regions involved in seizures at any stage and could be useful for clinical monitoring and surgical planning. The method's simplicity and strong performance suggest it is promising for the real-time application during epilepsy treatment.

**Keywords:** *Dynamic trajectory, electroencephalogram, recurrence plot, seizure*

Submitted: 08-Nov-2024

Revised: 03-Dec-2024

Accepted: 05-Dec-2024

Published: 10-Jul-2025

## Introduction

The surgical treatment of patients with drug-resistant focal epilepsy depends on precisely identifying the brain region responsible for seizures. For many years, the clinical gold standard for pinpointing this region has been through the use of intracranial electroencephalography recordings to detect the seizure onset zone. This zone is typically identified by visually inspecting the earliest changes in the electroencephalogram (EEG) traces or by detecting localized high-frequency activity at the start of a seizure.<sup>[1-4]</sup> Since seizures in a single patient can vary over time, recent studies have highlighted the significance of temporal and spatial changes in focal epilepsy.<sup>[4-9]</sup> A patient's spatiotemporal seizure dynamics can vary significantly, with the progression

of pathological activity, as observed in EEG recordings, differing from one seizure to another. Epilepsy is increasingly viewed as a dynamic disorder of the brain system.<sup>[10]</sup> Seizure evolutions can be described mathematical and statistical with various computational models.<sup>[4,7,11,12]</sup> Employing these methodologies, the progression of each seizure can be envisioned as a trajectory within the selected feature space. In addition, seizure prediction is more challenging in patients who have distinct populations of short and long seizures.<sup>[6]</sup> Brain discharge activity has the characteristics of transmission.<sup>[13-18]</sup> Brain functions as a complex network<sup>[9]</sup> with connections that are active during both static and dynamic activities. Investigating complex systems can provide a deeper comprehension of the complex dynamics underlying epileptic seizures. The recurrence of a specific activation sequence

This is an open access journal, and articles are distributed under the terms of the Creative Commons Attribution-NonCommercial-ShareAlike 4.0 License, which allows others to remix, tweak, and build upon the work non-commercially, as long as appropriate credit is given and the new creations are licensed under the identical terms.

For reprints contact: WKHLRPMedknow\_reprints@wolterskluwer.com

**How to cite this article:** Farahi M, Sajadi SS, Karbasi F, Fesharaki SS, Habibabadi JM, Haidari MR, *et al.* A nonlinear method to identify seizure dynamic trajectory based on variance of recurrence rate in human epilepsy patients using EEG. *J Med Signals Sens* 2025;15:19.

Morteza Farahi<sup>1</sup>,  
Seyed Saman Sajadi<sup>1,2</sup>,  
Fateme Karbasi<sup>1</sup>,  
Seyed Sohrab  
Hashemi Fesharaki<sup>3</sup>,  
Jafar Mehvari  
Habibabadi<sup>4</sup>,  
Mohsen Reza  
Haidari<sup>5</sup>,  
Amir Homayoun  
Jafari<sup>1,2</sup>

<sup>1</sup>Department of Medical Physics and Biomedical Engineering, School of Medicine, Tehran University of Medical Sciences, Tehran, Iran, <sup>2</sup>Research Center for Biomedical Technologies and Robotics, Tehran University of Medical Sciences, Tehran, Iran, <sup>3</sup>Pars Advanced Medical Research Centre, Pars Hospital, Tehran, Iran, <sup>4</sup>Isfahan Neuroscience Research Center, Isfahan University of Medical Sciences, Isfahan, Iran, <sup>5</sup>Section of Neuroscience, Department of Neurology, Faculty of Medicine, Baqiyatallah University of Medical Sciences, Tehran, Iran

**Address for correspondence:**  
Prof. Amir Homayoun Jafari,  
Department of Biomedical  
Engineering and Medical  
Physics, School of Medicine,  
Tehran University of Medical  
Sciences, Poursina Street,  
Tehran, Iran.  
E-mail: h\_jafari@tums.ac.ir

Supplementary Video available  
on: [www.jmssjournal.net](http://www.jmssjournal.net)

Access this article online

Website: [www.jmssjournal.net](http://www.jmssjournal.net)

DOI: 10.4103/jmss.jmss\_73\_24

Quick Response Code:



can be regarded as trajectories (oscillations) around an attractor point in the phase-space model of any dynamical system.<sup>[19,20]</sup> Disruptions in the neural network activation pattern (e. g., increased excitability, external stimuli, or varying inputs) can shift the system's trajectory, causing it to orbit a different attractor. The traditional repeating epileptiform activity pattern recorded from EEG or local field potentials leads may be the result of activating the same circuits in sequence, one after the other.<sup>[21]</sup> According to the discussion of electrographic signatures, the recurrent pattern of discharges observed in most epileptic convulsions clearly suggests that the same circuit sequence is frequently engaged. Whether this is due to a focal oscillating generator that initiates activity in downstream circuits,<sup>[22]</sup> a reverberant circuit providing positive feedback,<sup>[23]</sup> or a combination of both remains a topic of matter and may differ across different types of epilepsy within the spectrum. The recordings from epileptogenic areas were less random and more nonlinear dependent than those from nonepileptogenic areas.<sup>[24,25]</sup>

In 1987, Eckmann *et al.* invented the recurrence plot (RP), a nonlinear analysis technique, to show the fundamental dynamical properties of a dynamical system in the phase space.<sup>[26]</sup> A high-dimensional phase space trajectory was projected into a binary matrix, with the value set to 1 whenever two locations on the trajectory were sufficiently close together. This technique has been widely used to analyze the brain dynamics changes and transitions between states.<sup>[27-31]</sup> The potential patterns within RPs can be revealed through recurrence quantification analysis (RQA), a statistical quantification approach.<sup>[32]</sup> Recurrence analysis can objectively expose the dynamics underlying physiological data since it operates without making any assumptions.<sup>[33-38]</sup> RQA was reported to be effective in epilepsy analysis.<sup>[39-42]</sup> Over the past years, different measures based on RPs have been proposed and applied to the EEG to study epilepsy.<sup>[28,43-45]</sup> Similar tests also suggested that various epilepsy phases could be discriminated on the basis of dynamical features, which were employed in automatic categorization of EEG epochs or even the prediction of seizures<sup>[46-49]</sup> and different dynamical scenarios also implied different prospects for finding reliable control strategies.<sup>[50-52]</sup> Meanwhile, epileptic seizures are thought as the result of network disorder.<sup>[53-56]</sup> Therefore, it is necessary to investigating the dynamical interactions between stages as well as regions, and identifying the epileptogenic areas accordingly.

In this study, electroencephalograph (EEG) recordings from 17 patients were used, which directly recorded electrophysiological activity and clinicians report were considered as the gold standard for the epileptogenic region identification. The dynamical changes in different states and regions were revealed through quantification analysis of RPs. Epileptogenic areas were identified by nontrivial dynamical characteristics. Meanwhile, analysis of RPs was

used to demonstrate the recurrence phenomena between regions at different stages to identify simultaneous involved regions also the sequence of the involved areas in turn as seizure evolves. It is helpful for further understanding the role of epileptogenic areas from the epileptic network perspective, helping the deployment of new prediction and seizure abortion devices and surgical planning.

## Materials and Methods

### Participants

In this study, electroencephalograph (EEG) recordings from 17 patients with focal epilepsy, drug resistant and candidate for the surgical treatment were used (9 male,  $17.82 \pm 2.37$  years of age). All the participants were informed about the study and written informed consent was obtained before the data acquisition. The data were recorded at Pars hospital in Tehran and was approved by the Medical Research Ethics Committee of Tehran University of Medical Sciences and. Study design and data recording was done based on the Declaration of Helsinki. The demographic information of all participants is listed in Table 1. The data were acquired using the g. Hiamp MultiChannel Amplifier system. 32 EEG channel were recorded using 10-10 system at 500 Hz sampling frequency. A notch filter at 50 Hz and a bandpass filter between 0.5–100 Hz were applied during data acquisition. In total, 23 seizures belong to the anterior region among subjects, 47 seizures related to posterior regions, 16 seizures related to left temporal, and 9 for right temporal.

### Data analysis

After preprocessing the EEG data, quantification analysis of RPs showed the dynamical variations in various states and areas. Nontrivial dynamical features were used to identify epileptogenic zones. In the meantime, the recurrence phenomena between regions at various phases were demonstrated using the analysis of variance of RPs quantifications to identify concurrently involved regions as well as the order of the concerned areas in turn.

### Preprocessing

First, a IIR and Causal. 5-70 Hz Butterworth filter with order of 6 and minimum distortion was used to clean the recorded data. In order to analyze the patient's data, we divided the signals recorded from the patient in each seizure into three main parts; before seizure, during seizure and after seizure. The analysis starts from the preictal part and continues until the end of the postictal. Figure 1 shows the general process of the identification of trajectory of epileptic waves between the regions.

### Dynamic trajectory

Natural processes in general can show different recursive behavior. Returning behavior means when the state of the system converges after some time has passed, and this is a special feature of certain systems, including nonlinear

**Table 1: Demographics number of seizures of subjects enrolled in the study**

Subject	Age (mean±SD=17.82±2.37)	Gender (male: 9)	Symptom
S1	20	Female	Versive - dialeptic Electrographic
S2	22	Male	Visual aura - visual loss
S3	21	Male	Visual aura
S4	18	Female	Dialeptic
S5	14	Male	Versive - tonic - clonic
S6	16	Female	Versive - akinetic Clonic
S7	17	Male	Visual aura - dialeptic Tonic - clonic
S8	20	Male	Visual aura
S9	15	Male	Dialeptic - versive
S10	14	Male	Psychic aura Complex motor seizure
S11	17	Female	Visual aura - dialeptic Tonic - clonic
S12	19	Female	Visual aura Tonic
S13	18	Female	Visual aura - dialeptic Tonic - clonic
S14	16	Female	Discognitive - tonic - clonic Complex motor seizure
S15	17	Male	Visual aura - psychic aura
S16	17	Female	Hypermotor Visual aura
S17	20	Male	Tonic hypermotor Visual aura - automotor

SD – Standard deviation

and chaotic systems. The display of these returns can be done based on the analysis of the RPs. Hence, for the quantitative analysis of RPs, we aimed to focus on the rate of the recursion of states of the system.

The stages of the algorithm mentioned in this study are presented as following.

#### Calculation of the RP

First, delay parameters ( $\tau$ ) and embedding dimension ( $m$ ) are calculated with common information algorithm false nearest neighbors (FNNs), respectively, for the reconstruction of the phase space.<sup>[57]</sup>

The essential principle is that, even if they are not actual neighbors, a growing number of phase space points will be projected into the neighborhood of any phase space point as the dimension is decreased. We refer to these points as FNNs. The simplest approach determines the minimal embedding dimension by calculating the number of these FNNs as a function of the embedding dimension.<sup>[57,58]</sup> The dimension where the FNNs vanish must be taken. The ratios of the distances for different dimensions between the same nearby locations are used in other methods. The use of mutual information is a well-established technique for determining the delay.<sup>[58]</sup> It is the mean of the data regarding a value that may be obtained from the present value after a delay  $\tau$ . Where mutual information has the least local minimum is the ideal choice for the delay.

Next, we calculate the RP of system representing the brain signals. The RP is calculated using a square matrix  $R$  that contains the repetition or nonrepetition values of the system states.

$$R_{k,l}^{m, \varepsilon_i} = \theta(\varepsilon_i - \| \text{Brain signal}_k - \text{Brain signal}_l \|),$$

$$\text{Brain signal}_{k,l} \in R^m, \quad (1)$$

$$k, l = 1, 2, \dots, P.$$

In the equation 1,  $P$  is the number of considered states of  $x_k(t)$   $x_k(t)$ ,  $\| \cdot \|$  is the norm,  $\varepsilon_i$  the threshold limit and  $\theta$  the Heaviside function. More details on construction of RP's mentioned in.<sup>[57,58]</sup>

Since  $R_{k,k} = 1$  ( $k = 1, 2, \dots, N$ ) by definition, the RP has a black main diagonal line, the line of identity (LOI), with an angle of  $\pi/4$ . It has to be noted that a single recurrence points at  $(k, l)$  does not contain any information about the current states at the times  $k$  and  $l$ . However, from the totality of all the recurrence points, it is possible to reconstruct the phase space trajectory.

Therefore, a recurrence is defined as a state  $x_k$  that is sufficiently close to  $x_l$ . This means that those states  $x_k$  that fall into an  $m$ -dimensional neighborhood of size  $\varepsilon_i$  centered at  $x_l$  are recurrent. These  $x_k$  are called recurrence points.

Insights into the dynamics of dynamical systems can be gained via visual RPs. The drawback of graphical displays that lack the resolution to show RPs is that viewers must subjectively deduce and understand the patterns and structures that are displayed in the RP. In the early 1990s, Zbilut and Webber created definitions and processes to quantify RP structures in order to overcome the methodology's subjectivity.<sup>[32,59]</sup> They came up with the term RQA and created a set of recurrence variables that served as complexity metrics based on diagonal line structure in RPs.

$$RR_w = \frac{1}{P^2 - P} \sum_{k \neq l=1}^P R_{k,l}^{m, \varepsilon_i} \quad (2)$$

The equation 2, shows the recurrence rate (RR) coefficient of RP for each segmented window ( $w$ ) of 300 samples of

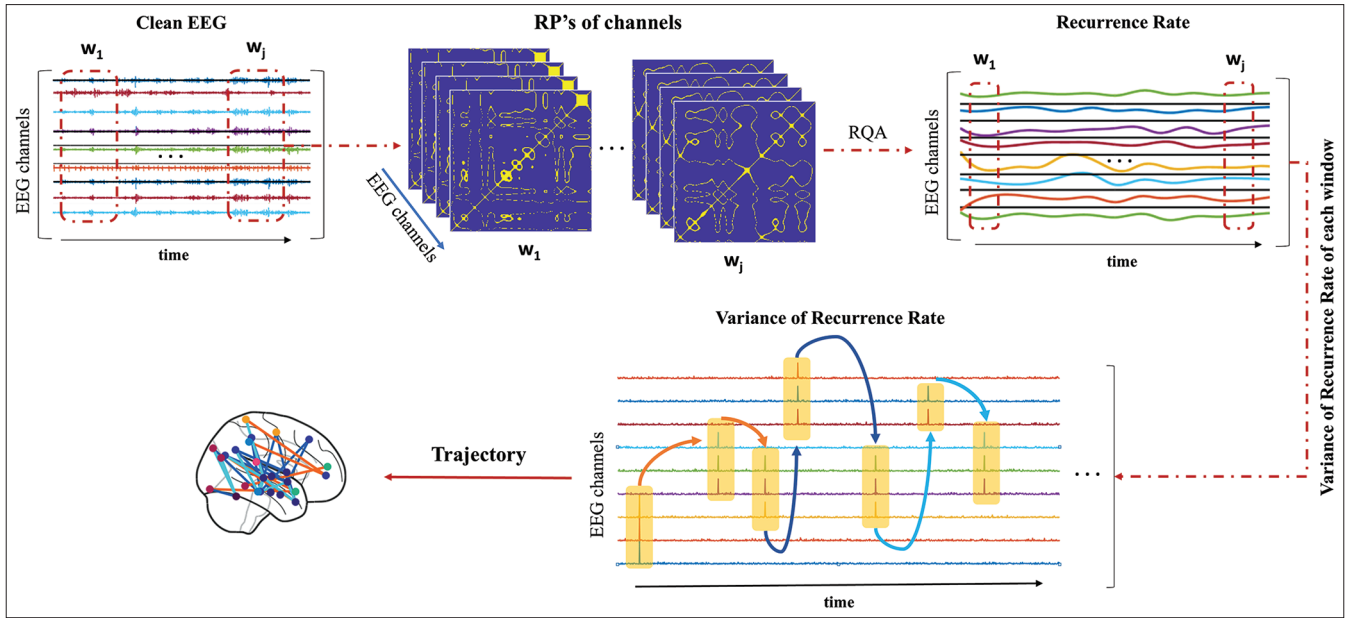


Figure 1: Graphical illustration of general block diagram of the nonlinear approach of extraction of trajectory map between epileptic regions

the brain signals used in this study (equation 1) which just counts or lists the black dots in the RP, omitting the LOI. It is associated with the definition of the correlation sum and represents the relative density of recurrence points in the sparse matrix.<sup>[32,58,59]</sup>

For the next step, we calculated the time of maximum RR relative to the start point of the seizure:

$$RR_i^{max} = \max(RR_i). \quad (3)$$

$$\tau_i = T_{RR_i^{max}} - T_{onset}. \quad (4)$$

In the equation 3,  $RR_i^{max}$  is the maximum of the vector of RR coefficients of each window in time for a single channel  $i = 1, 2, \dots, N$ . As shown in equation 4,  $\tau_i$  is the delay in reaching the maximum RR for the channel  $i$  from the onset.

Hence, in order to obtain the sequence of areas involved in seizure evolving using the obtained  $\tau_i$ , we can route delay as shown in equation 5:

$$\text{Trajectory Lag Index (TLI): } \text{Sort} \left\{ \begin{matrix} \max \\ \min \end{matrix} (\tau_i) \right\}. \quad (5)$$

The trajectory can be detected with the trajectory lag index (TLI) matrix. Here, we are not able to specify the involved areas and only the sequence of propagation of epilepsy between electrodes from the onset time and starting area could be detected. To detect the involved areas to shape the trajectory map as time evolves independent of the onset of seizure, we introduced the specific trajectory lag index (STLI) which will be explained in next section.

### Specific trajectory lag index

As explained in previous section, the TLI matrix could only identify the sequence of propagation of epilepsy

between electrodes. Another problem with TLI is that it is dependent to the onset of seizure to identify involved region only. We aimed to propose an approach to identify dynamic trajectory of seizure as time evolves independent of starting point. We hypothesized that there must be more variations in RR of involved regions comparing to noninvolved. Hence, we combined the analysis of variance and RR coefficients to strengthen the algorithm in the form of STLI. In this case, after calculating the RR as explained in the previous section, we calculated the variance on the RR coefficients in segments of time windows. Then, we continued the calculation process according to the variance values. The advantage of this method is that, in addition to the trajectory vector, it also determines the involved areas and the radius of the involvement with improved accuracy as time evolves but not depending on the seizure onset.

$$\overline{\sigma_j^{2RR}} = \frac{1}{N} \sum_{i=1}^N \sigma_{w_i}^{2RR} \cdot j = 1, 2, \dots, M, i = 1, 2, \dots, N. \quad (6)$$

In the equation 6,  $\overline{\sigma_j^{2RR}}$  is calculated on the vector of the variance of the RR coefficients in the specific window  $j$  with length of 12 samples for all channels.

$$S_{j,i} = \max(\sigma_{w_i}^{2RR}). \quad (7)$$

$$\text{Involvement area: } \{i\} = \sigma_{w_i}^{2RR} > \overline{\sigma_j^{2RR}} \ \& \ \sigma_{w_i}^{2RR} > 0.5 \times S_{j,i}. \quad (8)$$

As shown in equation 7,  $S_{j,i}$  shows the channel  $i$  with maximum variance of RR in  $j$ -th window. Then we used equation 8 to determine the involved area along with determining the radius of involvement around channel with maximum RR variance at each window. We used equation 9 to calculate the propagation delay between two consecutive time windows as STLI.

$$Special\ Trajectory\ Lag\ Index\ (STLI) : \Delta T = T_{S_{j+1}} - T_{S_j} \quad (9)$$

if  $i_{s_{j+1}} \neq i_{s_j}$ .

In equation 9, we can see that the result of a final vector includes the channels that are calculated as the main focus of epilepsy in each window  $w$ , and it can remain same or change during different windows. It is clear that the output of this method sometimes will show ping-pong swings in two channels or involvement radius around a centered channel, where the seizure center is temporarily stuck between two regions for a while.

In order to evaluate the results, we compared the detected areas with clinical reports for each subject to examine the similarities and differences in areas diagnosed by the algorithm and areas involved in epilepsy by the clinicians. The accuracy, sensitivity, and specificity along with Matthew’s correlation coefficient (MCC) and macro F1-score which is arithmetic mean (aka unweighted mean) of all the per-class F1 scores, were used as evaluation criteria.

$$Accuracy = \frac{TN + TP}{TN + TP + FN + FP} \quad (10)$$

$$Sensitivity = \frac{TP}{TP + FN} \quad (11)$$

$$Specificity = \frac{TN}{TN + FP} \quad (12)$$

$$MCC = \frac{TP * TN - FP * FN}{\sqrt{(TP + FP) * (TP + FN) * (TN + FP) * (TN + FN)}} \quad (13)$$

$$F1-score = \frac{2 * TP}{2 * TP + FP + FN} \quad (14)$$

Where:

True positive (TP): Involved EEG channel correctly classified as involved.

True negative (TN): Noninvolved EEG channel correctly classified noninvolved.

False positive (FP): Involved EEG channel wrongly classified as non-involved.

False negative (FN): Non-Involved EEG channel wrongly classified as involved.

Here, sensitivity is the ability to correctly identify seizure-involved regions and specificity is the ability to correctly identify non-involved regions. Accuracy shows correct predictions out of total predictions.

In the next part, the results of the proposed algorithm to find the trajectory of epilepsy and compare them with clinician’s reports will be mentioned.

## Results

In the previous section, we explained the TLI and STLI algorithms based on the analysis of variance of RR

coefficients extracted from the quantification analysis of RPs of each EEG channel as STLI.

In this section, we will show the results of nonlinear approach focusing on the RR parameter for identifying epileptic regions involved and dynamic trajectory of epilepsy evolution. First, based on this analysis, we calculated the amount of delay in the dynamic trajectory separately based on the variance of RR parameters of each channel in time windows. According to the obtained delay, we extract the trajectory map of involved regions in turn. Then, results of evaluation of the proposed algorithm will be shown in detecting epileptic areas with regard to the gold standard. As shown in Figure 2, we can see the RPs for two different EEG channels (P10 and PO8) at different stages before and after the ictal phase.

As shown in Figure 2, it is difficult to visually differentiate between the regions based on RPs. Thus, our focus was on examining the dynamic behavior of the brain using brain signal and their RPs and the quantity extracted from them.

In Figure 3a, we can see the result of RR coefficients in segments of EEG channels. Using the RRs, we calculated the active areas with a certain radius and then extract the line map over time using the RRs variance delay according to STLI algorithm. Figure 3b shows the result of analysis of variance of RR coefficients in time. Tracing peaks of variance of RRs in time between the channels, we could shape the trajectory map of involved areas in epileptic regions in turn as the time evolves.

According to the explanations given, finally, from the variance of the RR, we could obtain the propagation and occurrence of epilepsy among different brain regions over time. The results obtained from the STLI method do not depend on the time of onset of epilepsy and can be checked before its onset. The way epilepsy propagates, the simultaneity of the activity of the areas and the speed of its spread can depend on many factors [Figure 4]. Supplementary materials present the short videos of examples of visualization of epileptic propagation detection [Supplementary Videos 1 and 2].

As shown in Figure 4, the channels marked in black and shown in smaller size were not used during data acquisition

**Table 2: Comparison of results of specific trajectory lag index algorithm detected areas and clinicians report as gold standard**

Predicted by STLI algorithm	Expected by GOLD STANDARD			
	Anterior	Posterior	LT	RT
Anterior	20	1	0	2
Posterior	1	41	4	1
LT	2	1	12	1
RT	0	2	0	7

STLI – Specific Trajectory Lag Index; LT – Left temporal; RT – Right temporal

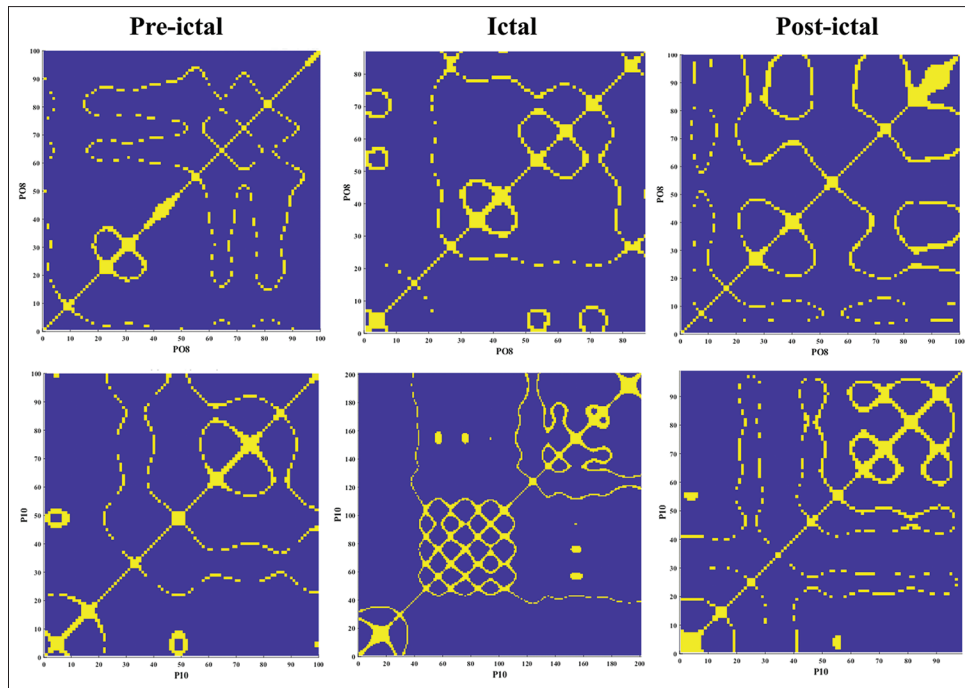


Figure 2: Results of recurrence plot of electroencephalogram (EEG). From left to right at pre-ictal, ictal and post-ictal for PO8 and P10, respectively

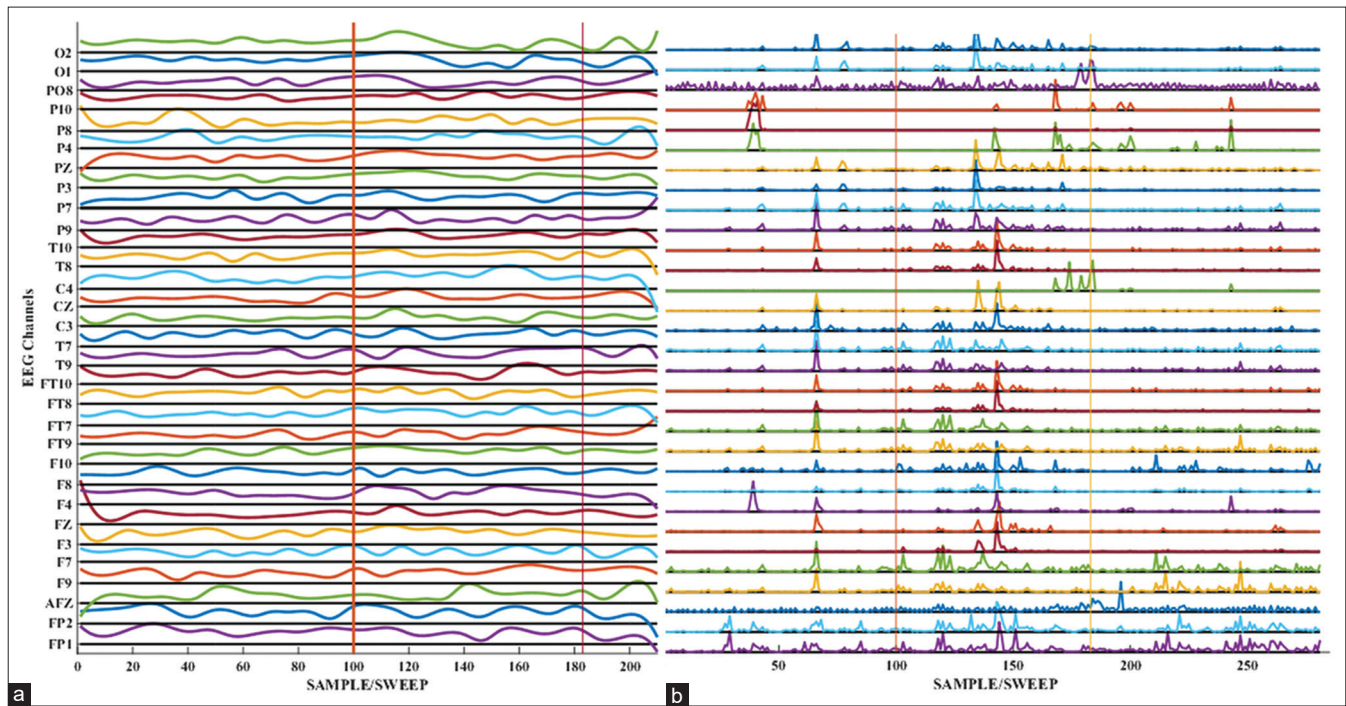


Figure 3: Quantification analysis of recurrence plots. (a) Recurrence rate (RR) coefficients of all channels, (b) Variance of RR coefficients. Vertical lines define pre-ictal, ictal and post-ictal stages in turn

from the patient. The remaining channels (yellow and green dots) were used to record the patient’s data in the study. The channels highlighted in green have been identified as seizure-involved regions by the STLI algorithm. The connections between these channels are illustrated by separate lines in three colors: red, blue, and pink, also extracted by the STLI algorithm. Pink lines represent the

connections during the preictal phase; red lines indicate connections during the ictal phase, and blue lines show connections during the postictal phase. These lines are plotted over time, allowing for observation of the temporal precedence and succession of these connections.

In order to validate the identified areas, it was necessary to perform a detailed statistical analysis. This analysis

included the comparison of the areas with expert clinician’s reports (gold standard) in the following. We estimated the regions based on four groups of location anterior, posterior, left temporal, and right temporal. Hence, in order for better comprehension of the comparison between predicted areas and areas labeled by the experts, we reformatted the whole confusion matrix of the four regions for each one of them [Table 2]. Figure 5 shows the performance of the algorithm to detect the regions involved in the process of preparation of seizure in the form of one vs all other regions.

As shown in Table 2, the algorithm has performed well in finding the epileptic regions according to the clinicians’

**Table 3: Results of comparison of regions detected by specific trajectory lag index and gold standards**

Subjects	Seizure onset region	Identified region based on STLI
S1	RT - LT - Frontotemporal	A-P-RT
S2	Posterior	P-RT
S3	Posterior	LT-P
S4	Posterior	P-P-A
S5	Anterior - posterior	A-P-LT
S6	Posterior	P-P-RT
S7	RT - LT - occipital	LT-P-P
S8	RT - LT	LT-RT-P
S9	Posterior	P-P-RT
S10	RT	P-RT-A-P
S11	Left occipital	P-LT-P-P
S12	Posterior	P-RT-P
S13	RT - LT	LT-P-LT-RT
S14	Posterior	P-A-LT
S15	RT - LT - posterior	LT-P-LT
S16	Right side	P-RT-P
S17	Left posterior temporal	P-A-P

P – Posterior; A – Anterior; LT – Left temporal; RT – Right temporal; STLI – Specific Trajectory Lag Index

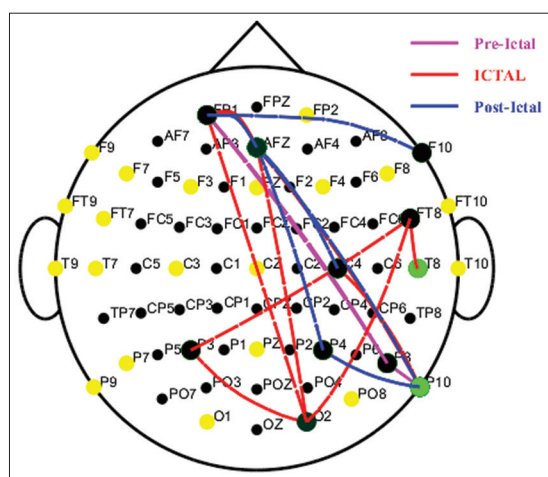


**Figure 4: Trajectory and areas involved in epilepsy based on specific trajectory lag index. The image depicts the distribution of electroencephalogram (EEG) channels on the scalp, with each channel represented by a dot, accompanied by its respective label**

report. Furthermore, according to Figure 5, we can see that the performance of the algorithm in all areas and their differentiation from each other is also acceptable. Based on the demographics of the patients, the number of people with temporal areas (left temporal (LT) and right temporal (RT)) involved in seizure is less than the others regions, which shows the presence of more errors in the misdiagnosis of these areas compared to the other areas. Table 3 shows the demographics of regions detected compared to the regions based on the clinical report onset region.

Based on this analysis, we calculated the amount of delay in the dynamic trajectory separately for each channel. Based on the obtained delay, we extracted and drew the trajectory map of involved areas in turn [Figure 4].

Hence, the proposed STLI method could investigate the involved areas considering their dynamical behaviors regarding to the analysis of variance of quantification calculated from each RPs of EEG channels.

### Discussion

In this translational study, we aimed to develop a method considering the complex and nonlinear behavior of the brain in epilepsy to investigate the brain regions involved in such a way that both the start and end points of the seizure can be displayed accurately and also the path of the signal trajectory during the development of the epileptic signal. In the previous sections, we were able to obtain the areas involved in the development of epileptic seizure with the resolution of one electrode by using the quantitative analysis of RPs. We focused on quantifications of RPs to better investigate the dynamical changes during propagation of epileptic waves. We mainly focused on the RR in RPs as we hypothesized that we must see shared dynamic behaviors of regions as seizure propagates which will be recurrent in different other regions in time or remain steady in a single region for a while. As shown in Figure 3a, the RR coefficients for each EEG channel that it did not differ between different regions as seizure

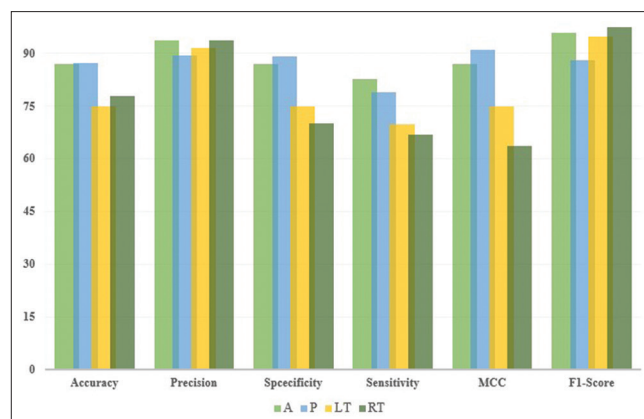


**Figure 5: Results of specific trajectory lag index method for detecting regions involved in seizure**

propagates in time and can only detect the regions involved from onset point based on sorting channels in reaching maximum RR quickly. However, analysis of variance of RR coefficients in time windows shows significant changes in between specific channels [Figure 3b]. Thus, as it was explained for equation 8 that we are able to determine the radii of involvement of neighboring channels of a region at each time. Our findings thus lend credence to the growing theory that rhythmic activity during seizures may have spread from a focal source in numerous brain regions.

Besides, the evaluations of the results of the STLI method with clinician's report as our gold standard were acceptable to detect epileptic regions during seizure. Figure 5 shows the performance of the algorithm to detect the regions involved in the process of preparation of seizure in the form of one versus all other regions. We can demonstrate that the accurate performance could be achieved for discerning involved and noninvolved regions in seizure propagation with 95.54 macro averaged F-score. For the anterior region, it achieved an overall accuracy of (0.86, 0.87), sensitivity of (0.82, 0.83), and specificity of (0.86, 0.87) and for posterior, right temporal and left temporal the STLI had (accuracy = [0.87, 0.87], sensitivity [0.78, 0.79], specificity = [0.88, 0.89]), (accuracy = [0.77, 0.77], sensitivity = [0.66, 0.67], specificity = [0.69, 0.70]), (accuracy = [0.74, 0.75], sensitivity = [0.69, 0.70], specificity = [0.74, 0.75]), respectively with 95% confidence interval. Our results show less accurate performance in LT and RT [Figure 5] regions. It can be caused by lack of seizure numbers that has been reported while engaging these two areas as explained in previous sections and so the misdetection of these two areas leads to more error values compared to other regions as we can see that can be seen as low MCC for temporal areas. The proposed STLI method can be used to analyze the signal from preictal stage to postictal to detect seizure onset and trajectory of involved areas in time for better understanding of seizure occurrence [Figure 4].

In this study, we aimed to detect the dynamic trajectory of seizure spread. As explained, we hypothesized that using quantification analysis of RPs as a nonlinear approach focusing on recurrence of seizure spread shared similar dynamics between regions. Thus, we could identify involved areas as the time progressed. Many researches have used this technique such as RQA and phase synchronization to identify the seizure stages or classifying healthy subjects.<sup>[60-63]</sup> Some studies have reported that RQA parameters derived from the RP are useful to categorize the EEG signal information as pre-ictal, ictal and normal categories.<sup>[62-65]</sup> RP is a sophisticated nonlinear data analysis method, and its RQA parameters calculate the signals' salient characteristics.<sup>[61]</sup> Our results are in line with other studies about the ability of RR coefficient in tracking the dynamic changes of brain electrical activity during seizure.<sup>[66-71]</sup> Although RR can identify seizure type

or stage, but it alone cannot identify trajectory of seizure spread as discussed earlier. The RR alone can only be used to identify set of EEG electrodes that are involved in seizure propagation or in another words, electrodes that receive shared dynamical behavior in turn. Therefore, we could not observe the difference in time in the RR values because their averages were almost close to each other at different time windows at specific stage to form the trajectory. For this, we must know onset and sort the time of reaching to maximum RR between channels as the TLI method (equation 5). Results of STLI method shows that it is the variations of RR that can identify involved regions in time. To put it more clearly, when an electrode involves in the trajectory of seizure propagation, its state is more recurrent than times before or after of it so at that time window, the variance of RR rises. Our approach differs considerably from standard neurophysiological measures of seizure onset in that they rely on phase differences in low-frequency or high gamma activity.<sup>[72-74]</sup> The problem with approaches relying on phase transition or locking is that first as a linear approach they might not be able to capture nonlinear and complex behavior of brain activity during seizure spread and needs simplified assumptions for modeling. Second, the frequency-based approaches with phase differences are limited by spatial aliasing and requires low frequency input to avoid ambiguity.<sup>[75]</sup> Furthermore, there might be contradictory findings on how fast or slow oscillations are propagating between the patients with focal epilepsy. Seizures may remain more focal for much longer than has previously been understood or suggested by clinical interpretations of the EEG recordings.<sup>[72,73,75]</sup> Our method, which is based on examining changes in the dynamical behaviors of such a nonlinear system, which may be regarded as a reliable methodology for seizure initiation and spread investigation differs significantly from conventional neurophysiological measurements of seizure detection. As already mentioned, it is extremely sensitive and difficult to identify active and implicated epileptic regions in drug-resistant patients who need a particular brain region surgically removed. Given the nonlinear nature of brain and the dynamic behavior of epileptic waves between different areas, there is a possibility of error in removing the epileptic onset area. Thus, the interpretability and simplicity of our model may be one of its strengths due to less computational demands comparing to recent proposed approaches to identify seizure dynamic behavior between different brain regions based on linear approaches or source reconstruction methods which requires more computational demands or invasive data.<sup>[63,75-79]</sup> Therefore, the simplicity of computation for implementation and reliance on nonlinear brain signal processing methods, indicate the high potential of our method for clinical applications and real-time monitoring even during epilepsy surgery to reduce the error in diagnosing the onset area and the area intended for surgery and matching clinical symptoms with the areas of the brain involved during an epileptic seizure for better

treatment. Our data provide support for the hypothesis that the source of pathologic activity can change location over the course of the seizure and is in fact a dynamic entity.<sup>[72-75]</sup> In accordance with clinical observations, animal models, and computer simulations, our data further indicate that the seizure source may occasionally even divide into several separate entities [Figure 4, green dots].<sup>[80-82]</sup> However, we cannot rule out the idea that what seem to be two different sources could actually be one source sending traveling waves to different cortical locations. Our findings imply that the seizure source might be dynamic, that the mechanisms controlling its movement and dissemination are not yet understood by conventional clinical interpretations or simplified modeling approaches, and that they might differ among patients with various underlying etiologies and seizure locations. The increasing recruitment of bigger brain regions may lead the seizure source to move. This recruitment may occur locally along the cortical sheet or distantly via white matter pathways, maybe even including the subcortical regions.<sup>[19,83-86]</sup> As the traveling waves' direction of propagation varies in each of these scenarios, the source's position may appear more diffuse. However, we found that within a single patient, this migration is comparatively stereotyped across seizures. The locations identified by our algorithm and clinical reports may differ in some ways due to the aforementioned factors [Tables 2 and 3]. Although we were limited to using clinical reports to assess our findings in this case, it is possible that the aforementioned issues such as source instability and dispersion and dynamic behavior could also skew the standard clinical interpretation. In the current study, we did not consider seizure type since we had lack of subjects due to difficulty of recording long term EEG data in clinic. Another consideration that should be pointed out is that here we detected switching between regions based on the changing in variance of RR between channels which occurs with a time delay as other researches mentioned also.<sup>[73-75,86]</sup> Another possible challenge in these studies can be the way to choose the number of brain signal recording channels, considering that their complex dynamic behavior in propagation requires more spatial resolution. In future studies, it is necessary to investigate the dynamic trajectory of seizure spread and the time delay of these transitions considering type of epilepsy, brain region or gender and other characteristics of the patients with more subjects and high-density EEG.

## Conclusion

In this study, we aimed to provide a method to investigate the dynamic trajectory and distribution of seizure with a nonlinear approach in patients with epilepsy. The described method determines the areas of brain involved seizure and the radius of involvement at any moment, and it is not dependent on the condition of the onset of epilepsy, but it can start investigating before the ictal and also determine

the moment of onset. It is possible to use the STLI method in the clinical monitoring and detection of seizure due to its simplicity in implementation for online application and promising results of this study.

## Financial support and sponsorship

This study is funded by the Tehran University of Medical Sciences with grant no. 403221345002.

## Conflicts of interest

There are no conflicts of interest.

## References

1. Kawai K. Epilepsy surgery: current status and ongoing challenges. *Neurol Med Chir* 2015;55:357-66.
2. Elger CE, Hoppe C. Diagnostic challenges in epilepsy: Seizure under-reporting and seizure detection. *Lancet Neurol* 2018;17:279-88.
3. Gracia CG, Chagin K, Kattan MW, Ji X, Kattan MG, Crotty L, *et al.* Predicting seizure freedom after epilepsy surgery, a challenge in clinical practice. *Epilepsy Behav* 2019;95:124-30.
4. Schroeder GM, Diehl B, Chowdhury FA, Duncan JS, de Tisi J, Trevelyan AJ, *et al.* Seizure pathways change on circadian and slower timescales in individual patients with focal epilepsy. *Proc Natl Acad Sci U S A* 2020;117:11048-58.
5. Saggio ML, Crisp D, Scott JM, Karoly P, Kuhlmann L, Nakatani M, *et al.* A taxonomy of seizure dynamotypes. *Elife* 2020;9:e55632.
6. Cook MJ, Karoly PJ, Freestone DR, Himes D, Leyde K, Berkovic S, *et al.* Human focal seizures are characterized by populations of fixed duration and interval. *Epilepsia* 2016;57:359-68.
7. Karoly PJ, Kuhlmann L, Soudry D, Grayden DB, Cook MJ, Freestone DR. Seizure pathways: A model-based investigation. *PLoS Comput Biol* 2018;14:e1006403.
8. Salami P, Peled N, Nadalin JK, Martinet LE, Kramer MA, Lee JW, *et al.* Seizure onset location shapes dynamics of initiation. *Clin Neurophysiol* 2020;131:1782-97.
9. Salami P, Borzello M, Kramer MA, Westover MB, Cash SS. Quantifying seizure termination patterns reveals limited pathways to seizure end. *Neurobiol Dis* 2022;165:105645.
10. Yu H, Cai L, Wu X, Song Z, Wang J, Xia Z *et al.* Investigation of phase synchronization of interictal EEG in right temporal lobe epilepsy. *Physica A Stat Mech Appl* 2108;492:931-40.
11. Burns SP, Santaniello S, Yaffe RB, Jouny CC, Crone NE, Bergey GK, *et al.* Network dynamics of the brain and influence of the epileptic seizure onset zone. *Proc Natl Acad Sci U S A* 2014;111:E5321-30.
12. Van Mierlo P, Carrette E, Hallez H, Vonck K, Roost DV, Boon P, *et al.* Accurate epileptogenic focus localization through time-variant functional connectivity analysis of intracranial electroencephalographic signals. *Neuroimage* 2018;56:1122-33.
13. Nevado-Holgado AJ, Marten F, Richardson MP, Terry JR. Characterising the dynamics of EEG waveforms as the path through parameter space of a neural mass model: Application to epilepsy seizure evolution. *Neuroimage* 2012;59:2374-92.
14. Wendling F, Bartolomei F, Bellanger JJ, Chauvel P. Epileptic fast activity can be explained by a model of impaired GABAergic dendritic inhibition. *Eur J Neurosci* 2002;15:1499-508.
15. Jirsa VK, Stacey WC, Quilichini PP, Ivanov AI, Bernard C. On the nature of seizure dynamics. *Brain* 2014;137:2210-30.

16. Spencer SS, Spencer DD, Williamson PD, Mattson RH. Ictal effects of anticonvulsant medication withdrawal in epileptic patients. *Epilepsia* 1981;22:297-307.
17. Rossi GF, Colicchio G, Scerrati M. Resection surgery for partial epilepsy. Relation of surgical outcome with some aspects of the epileptogenic process and surgical approach. *Acta Neurochir (Wien)* 1994;130:101-10.
18. Schmeiser B, Zentner J, Steinhoff BJ, Brandt A, Schulze-Bonhage A, Kogias E, *et al.* The role of presurgical EEG parameters and of reoperation for seizure outcome in temporal lobe epilepsy. *Seizure* 2017;51:174-9.
19. Martinet LE, Ahmed OJ, Lepage KQ, Cash SS, Kramer MA. Slow spatial recruitment of neocortex during secondarily generalized seizures and its relation to surgical outcome. *J Neurosci* 2015;35:9477-90.
20. Farooque P, Duckrow R. Subclinical seizures during intracranial EEG recording: Are they clinically significant? *Epilepsy Res* 2014;108:1790-6.
21. Schindler KA, Bialonski S, Horstmann MT, Elger CE, Lehnertz K. Evolving functional network properties and synchronizability during human epileptic seizures. *Chaos* 2008;18:033119.
22. Izhikevich EM. *Dynamical Systems in Neuroscience: The Geometry of Excitability and Bursting*: MIT Press; 2007.
23. Lopes da Silva F, Blanes W, Kalitzin SN, Parra J, Suffczynski P, Velis DN. Epilepsies as dynamical diseases of brain systems: Basic models of the transition between normal and epileptic activity. *Epilepsia* 2003;44 Suppl 12:72-83.
24. Nganga EJ, Bialonski S, Marwan N, Kurths J, Geier C, Lehnertz K. Evaluation of selected recurrence measures in discriminating pre-ictal and inter-ictal periods from epileptic EEG data. *Phys Lett A* 2016;380:1419-25.
25. Andrzejak RG, Schindler K, Rummel C. Nonrandomness, nonlinear dependence, and nonstationarity of electroencephalographic recordings from epilepsy patients. *Phys Rev E Stat Nonlin Soft Matter Phys* 2012;86:046206.
26. Eckmann JP, Kamphorst SO, Ruelle D. Recurrence plots of dynamical systems. *Europhys Lett* 1987;4:973-7.
27. Goshvarpour A, Abbasi A, Goshvarpour A. Dynamical analysis of emotional states from electroencephalogram signals. *Biomed Eng Appl Basis Commun* 2016;28:1650015.
28. Subramaniam NP, Hyttinen J. Analysis of Nonlinear Dynamics of Healthy and Epileptic EEG Signals Using Recurrence Based Complex Network Approach. In: 2013 6<sup>th</sup> International IEEE/EMBS Conference on Neural Engineering (NER). IEEE; 2013. p. 605-8.
29. Pitsik E, Frolov N, Hauke Kraemer K, Grubov V, Maksimenko V, Kurths J, *et al.* Motor execution reduces EEG signals complexity: Recurrence quantification analysis study. *Chaos* 2020;30:023111.
30. Marwan N, Romano MC, Thiel M, Kurths J. Recurrence plots for the analysis of complex systems. *Phys Rep* 2007;438:237-329.
31. Marwan N, Kurths J, Foerster S. Analysing spatially extended high-dimensional dynamics by recurrence plots. *Phys Lett A* 2015;379:894-900.
32. Webber CL Jr., Zbilut JP. Dynamical assessment of physiological systems and states using recurrence plot strategies. *J Appl Physiol (1985)* 1994;76:965-73.
33. Marwan N, Kurths J. Nonlinear analysis of bivariate data with cross recurrence plots. *Phys Lett A* 2002;302:299-307.
34. Perc M. Nonlinear time series analysis of the human electrocardiogram. *Eur J Phys* 2005;26:757-68.
35. Narin A, Isler Y, Ozer M, Perc M. Early prediction of paroxysmal atrial fibrillation based on short-term heart rate variability. *Physica A* 2018;509:56-65.
36. Perc M. The dynamics of human gait. *Eur J Phys* 2005;26:525-34.
37. Ginoux J, Ruskeepää H, Perc M, Naeck R, Costanzo DV, Bouchouicha M, *et al.* Is type 1 diabetes a chaotic phenomenon? *Chaos Solitons Fractals* 2018;111:198-205.
38. Tatum WO, Rubboli G, Kaplan PW, Mirsafari SM, Radhakrishnan K, Gloss D, *et al.* Clinical utility of EEG in diagnosing and monitoring epilepsy in adults. *Clin Neurophysiol* 2018;129:1056-82.
39. Chandrasekharan S, Jacob JE, Cherian A, Iype T. Exploring recurrence quantification analysis and fractal dimension algorithms for diagnosis of encephalopathy. *Cogn Neurodyn* 2024;18:133-46.
40. Goel S, Agrawal R, Bharti RK. Automated detection of epileptic EEG signals using recurrence plots-based feature extraction with transfer learning. *Soft Comput* 2024;28:2367-83.
41. Bernardo D, Kim J, Cornet MC, Numis AL, Scheffler A, Rao VR, *et al.* Machine learning for forecasting initial seizure onset in neonatal hypoxic-ischemic encephalopathy. *Epilepsia* 2024. [doi: 10.1111/epi.18163].
42. Li JW, Feng GY, Lv JJ, Chen RJ, Wang LJ, Zeng XX, *et al.* A rhythmic encoding approach based on EEG time-frequency image for epileptic seizure detection. *Biomed Signal Process Control* 2025;99:106824.
43. Andrade KC, Wehrle R, Spoomaker VI, Sämman PG, Czisch M. Statistical evaluation of recurrence quantification analysis applied on single trial evoked potential studies. *Clin Neurophysiol* 2012;123:1523-35.
44. Ouyang G, Li X, Dang C, Richards DA. Using recurrence plot for determinism analysis of EEG recordings in genetic absence epilepsy rats. *Clin Neurophysiol* 2008;119:1747-55.
45. Yan J, Wang Y, Ouyang G, Yu T, Li X. Using max entropy ratio of recurrence plot to measure electrocorticogram changes in epilepsy patients. *Physica A* 2016;443:109-16.
46. Madeo D, Castellani E, Santarcangelo EL, Mocenni C. Hypnotic assessment based on the recurrence quantification analysis of EEG recorded in the ordinary state of consciousness. *Brain Cogn* 2013;83:227-33.
47. Li X, Ouyang G, Yao X, Guan X. Dynamical characteristics of pre-epileptic seizures in rats with recurrence quantification analysis. *Phys Lett A* 2004;333:164-71.
48. Acharya UR, Sree SV, Chattopadhyay S, Yu W, Ang PC. Application of recurrence quantification analysis for the automated identification of epileptic EEG signals. *Int J Neural Syst* 2011;21:199-211.
49. Kalitzin SN, Velis DN, da Silva FH. Stimulation-based anticipation and control of state transitions in the epileptic brain. *Epilepsy Behav* 2010;17:310-23.
50. Wang P, Wang D, Lu J. Controllability analysis of a gene network for *Arabidopsis thaliana* reveals characteristics of functional gene families. *IEEE/ACM Trans Comput Biol Bioinform* 2018. [doi: 10.1109/TCBB.2018.2821145].
51. Xu S, Wang P, Zhang CX, Lu J. Spectral learning algorithm reveals propagation capability of complex networks. *IEEE Trans Cybern* 2019;49:4253-61.
52. Naro D, Rummel C, Schindler K, Andrzejak RG. Detecting determinism with improved sensitivity in time series: Rank-based nonlinear predictability score. *Phys Rev E Stat Nonlin Soft Matter Phys* 2014;90:032913.
53. Andrzejak RG, Widman G, Lehnertz K, Rieke C, David P, Elger CE. The epileptic process as nonlinear deterministic dynamics in a stochastic environment: An evaluation on mesial temporal lobe epilepsy. *Epilepsy Res* 2001;44:129-40.
54. Cleeren E, Premereur E, Casteels C, Goffin K, Janssen P, Van

- Paesschen W. The effective connectivity of the seizure onset zone and ictal perfusion changes in amygdala kindled rhesus monkeys. *Neuroimage Clin* 2016;12:252-61.
55. Terry JR, Benjamin O, Richardson MP. Seizure generation: The role of nodes and networks. *Epilepsia* 2012;53:e166-9.
  56. Khambhati AN, Davis KA, Oommen BS, Chen SH, Lucas TH, Litt B, *et al.* Dynamic network drivers of seizure generation, propagation and termination in human epilepsy. *PLoS Comput Biol* 2015;11:e1004608.
  57. Marwan N, Romano MC, Thiel M, Kurths J. Recurrence plots for the analysis of complex systems. *Phys Rep* 2007;438:237-329.
  58. Webber CL, Marwan N. Recurrence Quantification Analysis. Theory and Best Practices. 2015. p. 426. [doi: 10.1007/978-3-319-07155-8].
  59. Zbilut JP, Webber CL Jr. Recurrence quantification analysis: Introduction and historical context. *Int J Bifurcat Chaos* 2007;17:3477-81.
  60. Mao L, Zheng G, Cai Y, Luo W, Zhang Q, Peng W, *et al.* Frontotemporal phase lag index correlates with seizure severity in patients with temporal lobe epilepsy. *Front Neurol* 2022;13:855842.
  61. Nishiyama M, Iwai Y, Oguri M, Maegaki Y. Phase Lag Index Histogram Features for Identifying Epileptic Seizure EEG Signals. In: 2021 IEEE 10<sup>th</sup> Global Conference on Consumer Electronics (GCCE). IEEE; 2021. p. 141-4.
  62. Lin LC, Ouyang CS, Chiang CT, Yang RC, Wu RC, Wu HC. Cumulative effect of transcranial direct current stimulation in patients with partial refractory epilepsy and its association with phase lag index-a preliminary study. *Epilepsy Behav* 2018;84:142-7.
  63. Stam CJ, Nolte G, Daffertshofer A. Phase lag index: Assessment of functional connectivity from multi channel EEG and MEG with diminished bias from common sources. *Hum Brain Mapp* 2007;28:1178-93.
  64. Gruszczyńska I, Mosdorf R, Sobaniec P, Żochowska-Sobaniec M, Borowska M. Epilepsy identification based on EEG signal using RQA method. *Adv Med Sci* 2019;64:58-64.
  65. Akbarian B, Erfanian A. Automatic seizure detection based on nonlinear dynamical analysis of EEG signals and mutual information. *Basic Clin Neurosci* 2018;9:227-40.
  66. Niknazar M, Mousavi SR, Vahdat BV, Sayyah M. A new framework based on recurrence quantification analysis for epileptic seizure detection. *IEEE J Biomed Health Inform* 2013;17:572-8.
  67. Rangaprakash D, Pradhan N. Study of phase synchronization in multichannel seizure EEG using nonlinear recurrence measure. *Biomed Signal Process Control* 2014;11:114-22.
  68. Torse DA, Khanai R, Desai VV. Classification of Epileptic Seizures Using Recurrence Plots and Machine Learning Techniques. In: 2019 International Conference on Communication and Signal Processing (ICCSP). IEEE; 2019. p. 0611-5.
  69. Chen L, Zou J, Zhang J. Dynamic Feature Extraction of Epileptic EEG Using Recurrence Quantification Analysis. In: Proceedings of the 10<sup>th</sup> World Congress on Intelligent Control and Automation. IEEE; 2012. p. 5019-22.
  70. Khosla A, Khandnor P, Chand T. EEG-based automatic multi-class classification of epileptic seizure types using recurrence plots. *Expert Syst* 2022;39:e12923.
  71. Ranichitra A, Palanisamy V, Ellapparaj R. A differential biomarker based on recurrence quantification analysis of EEG signal and genetic algorithm for epilepsy diagnosis. *J Artif Intell Syst Model* 2024;1:75-87.
  72. Weiss SA, Banks GP, McKhann GM Jr., Goodman RR, Emerson RG, Trevelyan AJ, *et al.* Ictal high frequency oscillations distinguish two types of seizure territories in humans. *Brain* 2013;136:3796-808.
  73. Weiss SA, Lemesiou A, Connors R, Banks GP, McKhann GM, Goodman RR, *et al.* Seizure localization using ictal phase-locked high gamma: A retrospective surgical outcome study. *Neurology* 2015;84:2320-8.
  74. Wagner FB, Eskandar EN, Cosgrove GR, Madsen JR, Blum AS, Potter NS, *et al.* Microscale spatiotemporal dynamics during neocortical propagation of human focal seizures. *Neuroimage* 2015;122:114-30.
  75. Diamond JM, Withers CP, Chapeton JI, Rahman S, Inati SK, Zaghoul KA. Interictal discharges in the human brain are travelling waves arising from an epileptogenic source. *Brain* 2023;146:1903-15.
  76. van Mierlo P, Vorderwülbecke BJ, Staljanssens W, Seeck M, Vulliémot S. Ictal EEG source localization in focal epilepsy: Review and future perspectives. *Clin Neurophysiol* 2020;131:2600-16.
  77. Millán AP, van Straaten EC, Stam CJ, Nissen IA, Idema S, Baayen JC, *et al.* Epidemic models characterize seizure propagation and the effects of epilepsy surgery in individualized brain networks based on MEG and invasive EEG recordings. *Sci Rep* 2022;12:4086.
  78. Tong X, Wang J, Qin L, Zhou J, Guan Y, Zhai F, *et al.* Analysis of power spectrum and phase lag index changes following deep brain stimulation of the anterior nucleus of the thalamus in patients with drug-resistant epilepsy: A retrospective study. *Seizure* 2022;96:6-12.
  79. Hindriks R. Relation between the phase-lag index and lagged coherence for assessing interactions in EEG and MEG data. *Neuroimage Rep* 2021;1:100007.
  80. Proix T, Jirsa VK, Bartolomei F, Guye M, Truccolo W. Predicting the spatiotemporal diversity of seizure propagation and termination in human focal epilepsy. *Nat Commun* 2018;9:1-15.
  81. Smith EH, Liou JY, Davis TS, Merricks EM, Kellis SS, Weiss SA, *et al.* The ictal wavefront is the spatiotemporal source of discharges during spontaneous human seizures. *Nat Commun* 2016;7:11098.
  82. Liou JY, Smith EH, Bateman LM, Bruce SL, McKhann GM, Goodman RR, *et al.* A model for focal seizure onset, propagation, evolution, and progression. *Elife* 2020;9:e50927.
  83. Schevon CA, Weiss SA, McKhann G Jr., Goodman RR, Yuste R, Emerson RG, *et al.* Evidence of an inhibitory restraint of seizure activity in humans. *Nat Commun* 2012;3:1060.
  84. Liu M, Bernhardt BC, Hong SJ, Caldairou B, Bernasconi A, Bernasconi N. The superficial white matter in temporal lobe epilepsy: A key link between structural and functional network disruptions. *Brain* 2016;139:2431-40.
  85. Kim H, Piao Z, Liu P, Bingaman W, Diehl B. Secondary white matter degeneration of the corpus callosum in patients with intractable temporal lobe epilepsy: A diffusion tensor imaging study. *Epilepsy Res* 2008;81:136-42.
  86. Rossi LF, Wykes RC, Kullmann DM, Carandini M. Focal cortical seizures start as standing waves and propagate respecting homotopic connectivity. *Nat Commun* 2017;8:1-11.